Journal of Applied Polymer Science

# Study of the Effect of Processing Conditions on the Co-Injection of PBS/PBAT and PTT/PBT Blends for Parts with Increased Bio-Content

**Matthew Zaverl,[1] Oscar Valerio,[1,2] Manjusri Misra,[1,2] Amar Mohanty[1,2]**

[1]School of Engineering, University of Guelph, Ontario, Canada N1G 2W1

[2]Department of Plant Agriculture, Bioproducts Discovery and Development Center (BDDC), University of Guelph, Guelph, Ontario, Canada N1G 2W1

Correspondence to: M. Misra (E-mail: mmisra@uoguelph.ca)

**ABSTRACT:** This work studies the effect of processing parameters on mechanical properties and material distribution of co-injected polymer blends within a complex mold shape. A partially bio-sourced blend of poly(butylene terephthalate) and poly(trimethylene terephthalate) PTT/PBT was used for the core, with a tough biodegradable blend of poly (butylene succinate) and poly (butylene adipate-co-terephthalate) PBS/PBAT for the skin. A $^1/_2$ factorial design of experiments is used to identify significant processing parameters from skin and core melt temperatures, injection speed and pressure, and mold temperature. Interactions between the processing effects are considered, and the resulting statistical data produced accurate linear models indicating that the co-injection of the two blends can be controlled. Impact strength of the normally brittle PTT/PBT blend is shown to increase significantly with co-injection and variations in core to skin volume ratios to have a determining role in the overall impact strength. Scanning electron microscope images were taken of co-injected tensile samples with the PBS/PBAT skin dissolved displaying variations of mechanical interlocking occurring between the two blends. © 2014 The Authors Journal of Applied Polymer Science Published by Wiley Periodicals, Inc. J. Appl. Polym. Sci. **2015**, *132*, 41278.

**KEYWORDS:** biopolymers & renewable polymers; blends; mechanical properties; molding; morphology

Received 19 November 2013; accepted 7 July 2014

**DOI: 10.1002/app.41278**

## INTRODUCTION

Forecasts of depleted oil productions have prompted research into the field of bioplastics which are derived from renewable resources. The widespread use of biopolymers to fill the gap has, however, been hindered by a number of problems, the main concerns being both cost and performance.[1] In an effort to resolve these issues bioplastics have been studied with a focus on fillers,[1,2] reinforcements,[2,3] or blending.[4] Among the different solutions the advanced processing method such as co-injection molding (CIM) promises an effective way to resolve a number of the problems. Examining the processing parameters can provide a way to determine the effectiveness of using CIM of a blend of poly(butylene terephthalate) and poly(trimethylene terephthalate) (PBT/PBT) as the core material with a blend of poly (butylene succinate) and poly (butylene adipate-co-terephthalate) (PBS/PBAT).

There are many variations of CIM but the basic concept utilizes more than one separate polymer components through sequential or continuous injection. The Co-Injection process, also know as sandwich molding, was invented in the 1970 by Imperial Chemical Industries.[5,6] Sandwich molding is one method of molding under the co-injection process, and is done with the sequential injection of the materials involved. The final result is a heterogeneous product composed of two separate layers, one core layer and one encapsulating layer of skin material. Combining two materials in this fashion produces properties which are unrepeatable by a single homogeneous polymer blend. Strength and modulus' result from core material

properties, while impact strength, hardness, and other surface properties, are related to the skin material. Core material selection has historically been chosen to reduce costs through sourcing of recycled or cheaper polymers.[7,8] Furthermore the core can include reinforcements such as fibers or particles which have been known to improve upon the skin/core interface.[9,10]

Successful CIM of two different polymers is fundamental to the material compatibility. Materials must share similar thermal expansion and shrinkage to prevent delamination at the polymer-polymer interface. The presence of interfacial bonding, through either chemical adhesion or mechanical interlocking of the two interfaces, also contributes to a successful CIM product.[9] Appropriate material selection enables the proper distribution of the core within the skin material. Core distribution is highly dependent on the viscosities of the selected materials. It is generally accepted that the ratio of core to skin viscosity range from 0.5 to 5 for a successful co-injection of two separate materials.[11–13] To better understand the importance of viscosity it is best to consider the hydrodynamic interpretation of two phase flow in molds as presented by Young et al.[8] Under this model the two melt flow phases 1 and 2 are pictured to flow side by side while both filling the mold cavity. Mean velocity of each phase is explained as a Newtonian fluid.

$$\bar{v}_1 = \frac{H^2}{\eta_1}\nabla p_1 \quad (1)$$

$$\bar{v}_2 = \frac{H^2}{\eta_2}\nabla p_2 \quad (2)$$

Where $\bar{v}$ is the mean velocity, $H$ is the distance from the center of the fluid layer to the wall such that $2H$ is the thickness of the fluid layer, $\eta$ is the fluid viscosity, and $\nabla p$ is the pressure gradient experienced by the fluid, fluid, being the molten polymer. At the interface the pressures and pressure gradients are equal.

$$p_1 = p_1 \qquad \nabla p_1 = \nabla p_2$$

Thus at any interface position,

$$\eta_1\bar{v}_1 = \eta_2\bar{v}_2 \quad (3)$$

$$\frac{\bar{v}_2}{\bar{v}_1} = \frac{\eta_1}{\eta_2} \quad (4)$$

From this relation we can conclude that when $\eta_2 > \eta_1$ the more viscous polymer melt (2) will move slower than the less viscous melt (1). If the core melt viscosity ($\eta_2$) becomes increasing more viscous than the skin, $\eta_2 \gg \eta_1$ than the core material will have a low velocity and undergo low core penetration. As documented by many researchers certain processing parameters including melt temperature, mold temperature, injection speeds, and injection pressure have a large effect on the viscosities of the materials and thus a direct impact on the core and skin distribution.[7–16]

Much of the different material skin/core compatibility is focused on petroleum based polymers.[17] As previously discussed increasing attention has been brought to the field of biopolymers in the recent forecasts of petroleum depletion and increasing greenhouse gas emission. With the hopes of improving bio-content usage, the core layer material choice is a blend of poly (butylene terephthalate) (PBT) and poly(trimethylene terephthalate) (PTT) at 30 and 70 wt.%. The authors have previously studied the PTT/PBT (70/30 wt.%) blend.[18] In the previous study, variations in processing parameters and their effects on the mechanical properties, specifically notched Izod impact strength, was explored. Reasoning for the PTT/PBT blend was to keep costs lower while increasing bio-content for PBT applications by mixing it with PTT, which is sourced from bio-based 1,3-Propanediol and contains 37 wt.% of annually renewable plant-based content.[19] Regardless of the molding conditions this blend was found to be brittle and produced low notch Izod impact strengths. From this previous study it was found that the PTT/PBT blend contained one $T_g$, as a result of similar individual $T_g$'s prior to blending. The blend is considered to undergo fine scale intermeshing, a characteristic proposed by Run et al.[20] The fine level of entanglements forces the separate polymer constituents to act in a homogenous manner. This article proposes to increase the impact properties of the PTT/PBT blend by co-injecting it with a ductile blend of PBS, and PBAT. PBS is a biodegradable aliphatic polyester belonging to the poly (alkylene dicarboxylate) family, synthesized from succinic acid and 1, 4-butanediol by two-step process of esterification and deglycolization. PBS has a relatively high melting temperature ~150°C, excellent processing properties, and good thermal stability.[21,22] Pure PBS is limited by its low impact strength.[23] To overcome this problem researchers have focused on blending PBS with other aliphatic polyesters like poly(hydroxyl butyrate),[24] poly(ethylene oxide),[25] poly (butylene terephthalate),[25] and poly(butylene carbonate).[26] These blends with the exception of poly(butylene carbonate) have a detrimental effect on the biodegradability of PBS. PBAT is a well-known commercially popular biodegradable polymer. It is produced through the polycondensation of 1, 4-butanediol, adipic acid, and terephthalic acid. It has high elasticity, high elongation at break, resistance to wear, water, and oil, and has good processability.[27] The compatibility of PBAT with PLA has been a highly researched blend.[28–30] PBATs defining feature is its elongation property at 700% but contains relatively low tensile strength of 32 MPa.[31]

Blending PBS, which has good tensile strength but low impact strength, with PBAT, which has poor strength but excellent toughness, provides a potentially tough skin material for the CIM with the brittle PTT/PBT blend as the core. Blends of PBS/PBAT were studied by Jacob et al.[32] Formulations with a greater degree of PBS reported stronger tensile strengths, and crystallization percent, with a reduction in tensile elongation. PBS/PBAT blend was reported to be immiscible but produced a single $T_g$, which was because of the similar values of each polymers' respective $T_g$.[32] Successful molding of a tough PBS/PBAT blend as the skin layer in a biobased co-injection application has been previously studied by some of the current authors. In the previous study Zhang et al.[33] co-injected the tough PBS/PBAT to encapsulate a brittle composite of poly(hydroxybuturate-co-valerate) (PHBV) with natural fibers. They concluded

that co-injection with PBS/PBAT effectively increased the unnotched and notched Izod strengths as a function of skin thickness in the direction of the notch. The co-injection of PBS/PBAT skin is expected to increase the impact strength of the final product while maintaining a strong core from the PTT/PBT. The use of PBS/PBAT will soon further increase the bio-content of the entire co-injected formulation with the proposed release of PBS and PBAT produced from bio-sourced 1,4 butanediol.[35] In a mirror study to the previous publication of PTT/PBT blending,[19] the authors have focused on understanding the effects of varying the processing parameter on the properties of the co-injected samples. Rather than use the Taguchi Method for statistical modeling as done in the PTT/PBT blend study the authors utilized an analysis from a fractional factorial design of experiments (DOE) as suggested by Selene[8] and Vangosa.[14] With this method it is possible to consider interaction effects between parameters, which is not possible under the Taguchi analysis. Resulting fractional factorial design data indicate specific correlations between certain processing parameters and their effects on the final sample properties. These correlations are explained through basic parallel flow theory. Mechanical properties suggest there is some interaction between the skin and core layer.

## EXPERIMENTAL

### Materials

For this study PBT was supplied by Ticona in Florence, Kentucky, under the trade name Celanex grade 2000-3. PTT was supplied by DuPont in Delaware, USA, under the trade name Sorona. PBS (Biocosafe 1903) and PBAT (Biocosafe – 2003) were both supplied by Xinfu from China. Extruded materials and neat polymers were dried overnight at 80°C before processing.

### Processing Conditions

**Extrusion.** The PTT/PBT core and PBS/PBAT skin blends were prepared by a Leistritz co-rotating intermeshing twin screw extruder (MIC 27/aL-48) with a strand die. Pellets of PBT and PTT were hand mixed before processing at a 30/70 wt % ratio, respectively. Similarly PBS and PBAT were also hand mixed at a ratio of 60/40 wt.%. The Leistritz extruder has 10 temperature zones along the extruder barrel, with a 11th temperature on the die. The temperature profile for the core PTT/PBT blend was, from feed to die, 230°C–235°C −240°C −240°C–240°C–240°C −240°C–240°C–240°C −235°C–230°C. For blending PBS/PBAT the temperature profile was 130°C–140°C–145°C–150°C–150°C −150°C–150°C–150°C–150°C–145–140°C, screw speed was kept at 112 RPM for both blends. The extruded strands where subsequently cooled in a water bath before being chopped into pellets for co-injection.

**Molding.** Testing samples were created from one mold with a geometry that combined type IV tensile, flexural and Izod impact samples with dimensions based on ASTM standards, which are connected by runners from one gate entry. The molding was done in an ARBURG (Model No: 370 S &00–290/70, Germany) two unit injection molding machine, capable of both single and co-injection. Screw diameter in unit 1 was 35 mm with a temperature profile of 6 heating zones, while unit 2 screw diameters were 22 mm with five heating zones. Single injections were done using unit 1. The temperature profile for the single injection samples was 35°C–240°C–245°C–250°C–250°C–250°C from feed to nozzle for PTT/PBT blends and 35°C–185°C–190°C–190°C–190°C–190°C for PBS/PBAT. The CIM core material was PTT/PBT injected at two different temperature profiles depending on the experiment number; either 35°C–240°C–245°C–250°C–250°C–250°C or 35°C–230°C–235°C–240°C–240°C–240°C was used. The injection of the skin material of PBS/PBAT also had two different profiles, depending on the experiment number. Either 35°C–155°C–160°C–160°C–160°C or 35°C–185°C–190°C–190°C–190°C was used. For the remainder of the article the melt temperatures used during molding are denoted by the temperature used in the first zone of the barrel (240–250°C for the core and 160–190°C for the skin).

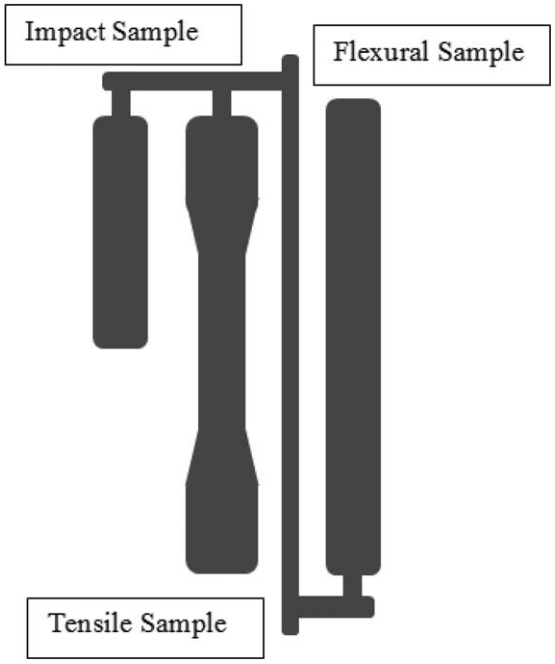


**Figure 1.** Three pronged mold design used in the co-injection study.

During CIM the skin blend was injected from unit 2, while the core was injected by unit 1. This allowed PTT/PBT, which has a higher processing temperature, to be injected by the larger barrel with a larger temperature profile. Skin to core volume ratio was chosen to be 60/40%, it should be noted that this is not the expected ratio to be found in the molded samples. Because of the complex nature of the mold geometry there is a length of runners that must be accounted for in determining the amount

**Table I.** Processing Parameters and Respected Levels

| Parameters | Low level | High level |
|---|---|---|
| Melt temperature (Skin) | 160°C | 190°C |
| Melt temperature (Core) | 240°C | 250°C |
| Mold temperature | 35°C | 50°C |
| Injection pressure | 500 PSI | 750 PSI |
| Injection speed | 10 cc/s | 20 cc/s |

**Table II.** Co-Injection 1/2 Factorial Design for PBS/PBAT and PTT/PBT

| | Melt temp (°C) (skin) | Melt temp (°C) (core) | Mold temp (°C) | Injection pressure (PSI) | Injection speed (PSI) |
|---|---|---|---|---|---|
| 1 | 160 | 240 | 50 | 500 | 10 |
| 2 | 190 | 240 | 35 | 500 | 10 |
| 3 | 160 | 240 | 35 | 500 | 20 |
| 4 | 190 | 240 | 50 | 500 | 20 |
| 5 | 190 | 250 | 50 | 750 | 20 |
| 6 | 190 | 240 | 50 | 750 | 10 |
| 7 | 160 | 240 | 35 | 750 | 10 |
| 8 | 160 | 240 | 50 | 750 | 20 |
| 9 | 160 | 250 | 35 | 750 | 20 |
| 10 | 160 | 250 | 35 | 500 | 10 |
| 11 | 160 | 250 | 50 | 500 | 20 |
| 12 | 190 | 250 | 35 | 750 | 10 |
| 13 | 160 | 250 | 50 | 750 | 10 |
| 14 | 190 | 250 | 50 | 500 | 10 |
| 15 | 190 | 240 | 35 | 750 | 20 |
| 16 | 190 | 250 | 35 | 500 | 20 |

of polymer accumulation in the final product. During the sequential injection molding a total of 28 cc is injected into the mold, thus 16.8 cc for skin and 11.2 cc for the core. The skin is injected first from unit 2 until 5 cc is left. The core material is then fully injected by unit 1 and then followed by the rest of the skin material. For the production of thinner impact samples a ratio of 40/60 vol % skin to core was used. In this setup skin was injected first from unit 2 until 3 cc was left. The core was then fully injected and followed up the remaining 3cc of skin polymer. Under this volume ratio the other testing specimens in the mold were unsuitable for testing because of core breakout.

A large determinant of the skin/core vol. ratio is the mold geometry. Much of the reported literature for experimental co-injection trials is done on a simple rectangular mold with either a center plate gate[8] or a lateral gate[36] while even fewer papers report co-injection results with complex shapes.[14] This research reports co-injection data from samples molded in a complex three-pronged geometry as seen in Figure 1.

For this reason there is an inability to fully encapsulate all three of the sample shapes. By focusing on fully encapsulating the tensile bar the flexural, and impact bars are left unfilled by the core, alternatively, by allowing the core to fully penetrate the flexural and impact samples the tensile bar experienced extensive core breakthrough. This problem was also experienced by Zhang et al.[33] Because of the nature of this research the skin/core ratio was chosen to allow for a full usage of all the samples. This was done by allowing the tensile sample to experience a restricted amount of core break, such that it did not extend into the narrow section of the sample. By ensuring that the narrow section was fully encapsulated, it could thus be assumed that the area under testing would be providing a proper representation of the tensile effects.

**Factorial Design.** To map the effects of variations in processing parameters a one half factorial design with level IV resolution, five factors and two levels was implemented. This allows interaction effects between two parameters to be studied under the assumption that three-way interactions are of no importance. The five factors consisted of processing parameters that could be manipulated on the ARBURG and are presented in Table I with their respected levels. The one half factorial is displayed in Table II. To better understand the role PBS/PBAT has on improving impact strength a second set of impact samples were created to have increased core content with a thinner skin encasement. For these samples a volume ratio of (40/60 vol %) skin to core ratio was used with a processing set as displayed in Table III. All analyses were done with the software Minitab® 16.

**Table III.** Processing Parameters for 40/60 Skin/Core Ratio Impact Samples

| Trial | Melt temp (°C) (skin) | Melt temp (°C) (core) | Mold temp (°C) | Injection pressure (PSI) | Injection speed (PSI) |
|---|---|---|---|---|---|
| 40/60 - 1 | 160 | 240 | 35 | 500 | 20 |
| 40/60 - 2 | 160 | 240 | 35 | 750 | 20 |
| 40/60 - 3 | 190 | 240 | 35 | 500 | 20 |
| 40/60 - 4 | 190 | 250 | 35 | 500 | 20 |

**Table IV.** Melt Flow Index of Skin and Core Blends

| Blend | MFI (g/ 10 min) | |
|---|---|---|
| PBS/PBAT | 19.7 ± 1.3 | (190°C, 2.16 kg) |
| PTT/PBT | 46.9 ± 1.1 | (250°C, 2.16 kg |

### Testing Methodologies

Tensile and Flexural tests were conducted on an Instron testing machine (Model-3382) according to ASTM standards D638 and D790, respectively, taking the average of five samples. Notched Izod impact strength was determined with a 5 ft-lb hammer on Testing Machine Inc (TMI 43-02) according to ASTM D256. For the testing of un-notched samples ASTM D256 was used with a 30 ft-lb hammer. Impact strength was taken as the average of seven samples. Melt flow index (MFI) was performed according to ASTM D1238 on a Qualitest Melt Flow Indexer (MFI-2000A) at the temperatures of 250°C for the PTT/PBT blend, and 190°C for the PBS/PBAT. The average value was taken from seven trials under a 2.16 kg weight.

### Characterization Methodologies

Changes in core/skin ratios were recorded from area profiles of cross sections of molded flexural samples. Cross sections were taken from the middle of flexural bars, and (+/−) 26 mm from the middle. These are aligned with all three contact points of a 3 pt. bending test. An average was taken from three different flexural bars for each cross section. To calculate the area, cross sections cut from the sample with a blade were analyzed under an optical microscope equipped with measurement software. The change in area was calculated as the ratio of area change between the cross section closest to the injection gate, and the cross section furthest away from the gate. The same method was used to characterize the skin thickness of the impact samples with cross sections taken from broken impact samples. The cross section was taken just under the break, and an average of the skin thickness on the notched side was taken from three cross sections. Scanning electron microscope (SEM) images were prepared using an Inspect S50 SEM at a high voltage of 20.000 kV. The samples were coated in gold before imaging for enhancing charge dissipation and preventing heat accumulation on the surface.

## RESULTS AND DISCUSSION

As previously described the overall goal of this article is to elucidate the behavior of the co-injection between both materials as a function of the processing parameters. Thus all mechanical data are paired with a statistical analysis to derive any possible trends that are occurring with the injection process.

To better explain the following discussion it must first be considered the effects that arise from the adjustment of various processing parameters. Much effort has been placed in relating the successful co-injection of two materials to the viscosity ratio between the materials under study.

To obtain proper mold filling it is recommended that the viscosity of the core material is higher than the skin viscosity. In this case the more viscous core can effectively push the remaining skin material to the end of the mold without breaking through and disrupting the skin encapsulation.[14–16] Previous studies have shown that the viscosity ratio $\eta_{core}/\eta_{skin}$ should be between 0.5 and 5.[36] Other sources have cited that optimal ratio between viscosities ranges between 0.8 and 1.8.[8] Young et al.[14]

**Table V.** ANOVA Analysis on DOE with Significant Terms Highlighted, and Removed Terms Asterisked

| | DF | Core penetration | Core difference | Impact skin thickness | Impact | Tensile strength | Flexural strength |
|---|---|---|---|---|---|---|---|
| Main Effects | 5 | 0 | 0 | 0.057 | 0.049 | 0 | 0 |
| Melt (skin) | 1 | **0.026** | 0.05 | **0.021** | 0.053 | 0.106 | 0.357 |
| Melt (core) | 1 | 0.591 | **0.026** | **0.04** | 0.122 | 0.131 | 0.574 |
| Mold | 1 | **0.009** | **0.028** | 0.187 | 0.05 | 0.075 | **0.022** |
| injection pressure | 1 | 0.942 | 0.294 | 0.204 | 0.121 | 0.983 | 0.731 |
| injection speed | 1 | **0.04** | 0.126 | **0.0149** | **0.027** | **0.042** | 0.776 |
| 2-Way Interactions | 8 | 0.06 | 0.03 | 0.038 | 0.049 | 0.008 | 0.057 |
| Melt(skin)*Melt(core) | 1 | 0.06 | * | 0.087 | * | 0.016 | * |
| Melt(skin)*Mold | 1 | **0.048** | * | 0.063 | 0.092 | * | 0.066 |
| Melt(skin)*injection pressure | 1 | **0.033** | 0.085 | * | **0.039** | **0.002** | * |
| Melt(skin)*injection speed | 1 | **0.029** | **0.033** | **0.031** | **0.024** | **0.037** | * |
| Melt(core)*Mold | 1 | 0.063 | 0.095 | * | **0.026** | 0.096 | 0.096 |
| Melt(core)*injection pressure | 1 | **0.024** | **0.039** | **0.019** | * | **0.017** | * |
| Melt(core)*injection speed | 1 | * | * | 0.074 | 0.183 | * | * |
| Mold*injection pressure | 1 | 0.08 | * | **0.049** | 0.15 | * | * |
| Mold*injection speed | 1 | **0.046** | **0.017** | 0.064 | 0.183 | * | **0.049** |
| injection pressure*injection speed | 1 | * | 0.097 | * | * | **0.027** | * |

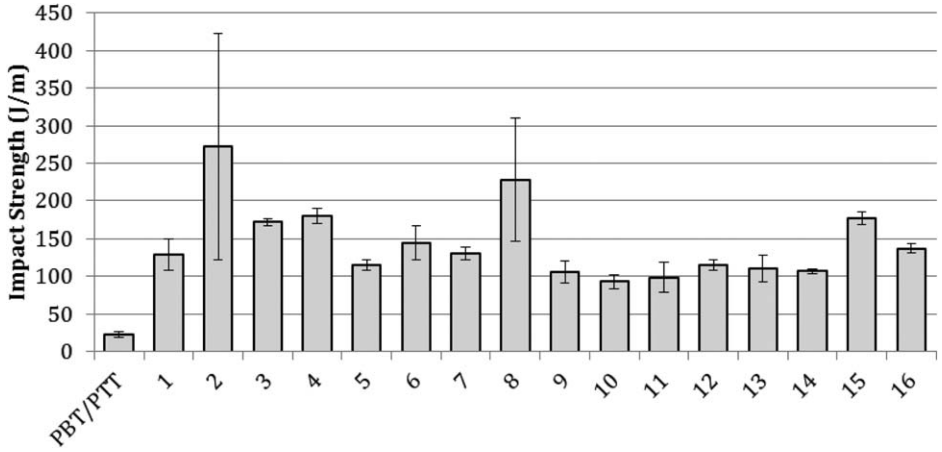


**Figure 2.** Impact Strengths of PTT/PBT and co-injected factorial DOE trials of PTT/PBT (40 vol %) with PBS/PBAT (60 vol %). Refer to Table II for processing parameters of trials 1–16.

report that greater skin uniformity occurs when the ratio of zero shear viscosities are between 1.5 and 2.0. MFI is directly related to material viscosity and is shown in Table IV.

Young et al.[14] compared multiple polymer parings for co-injection under varying viscosity ratios as they deviate from an optimal value. Viscosity ratios lower than the optimal value lead to a breakthrough of core material while higher ratios lead to poor mold filling. In the case of the lower ratios the skin material has a higher viscosity than the core. The lower viscosity of the core means the cores ability to evenly translate the pressure exerted from the injection of the core into the skin material is lost. Core material having a lower viscosity will accumulate and break through weaker points of the skin encapsulation, diminishing the heterogeneity between layers to be lost and forcing the sandwich injected part to be scrapped. Alternatively a large viscosity ratio is related to the core viscosity being much higher than the skins. Under these circumstances the ability of the skin material to contain the core material as its being injected is lost. Too low of a skin viscosity translates into an inability to contain the core material. Having no ability to resist the pressure from the incoming core polymer melt the majority of the skin material is pushed to the end of the mold, resulting in a nonuniformly distributed part in which most of the core is situated around the gate and the skin material is at the end furthest away from the gate.[8]

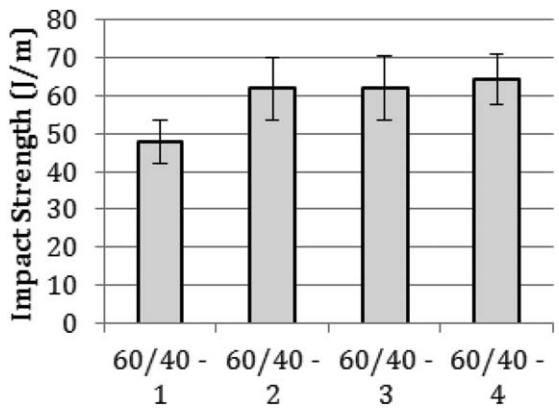


**Figure 3.** Notched impact strengths of co-injected PTT/PBT (70/30 wt %) [60 vol % injected] with PBS/PBAT (60/40 wt %) [40 vol % injected]. Refer to Table III for processing parameters of trials 1–4.

### ANOVA Analysis

Using a one half factorial design of experiments allowed for a statistical analysis between certain characteristics of the tested samples and the processing parameters used within each trial. Table V displays the *P*-values returned from ANOVA analysis done on different responses from the trials, with the significant terms highlighted, with significance taken as $\alpha = 0.05$. To improve upon the significance weighting of the parameters some largely insignificant interactions were removed from the ANOVA model. Doing this removed accuracy in the prediction model but allowed for the significant parameters and interactions to have a greater contrast. Three of the explored responses deal directly with the mold filling and core/skin ratio in design (core penetration in a flexural sample, core/skin ratio reduction along the profile of the flexural sample, and skin thickness at the notch of impact sample) while the other three characteristic responses deal with the mechanical strengths of the samples (impact, flexural, and tensile strengths). When performing an analysis with interaction terms, the interaction *P*-values are more important than the main effect *P*-values because of the reasoning that if the interaction is significant than a change in both processing parameters will affect the response characteristic regardless of the main effect significance. Comparing the significant interaction it is noted that the interactions "melt(core)* injection pressure" and "melt(skin)*injection speed" are significant for all characteristic responses in which they are present. This information leads to the observation that as the temperature of the melts change they are increasingly impacted by the injection process, which is an indication that there is a temperature dependency on the final properties. This can be related back to eq. (4), specifically the effect that temperature has on the viscosity of both polymer blends. In a previous factorial study on processing parameters, Selden[8] reported that core melt temperature and injection velocity had statistically significant effects on the skin/core distribution of co-injected polyamide (PA-6) as the skin and poly (butylene terephtalate) (PBTP) with

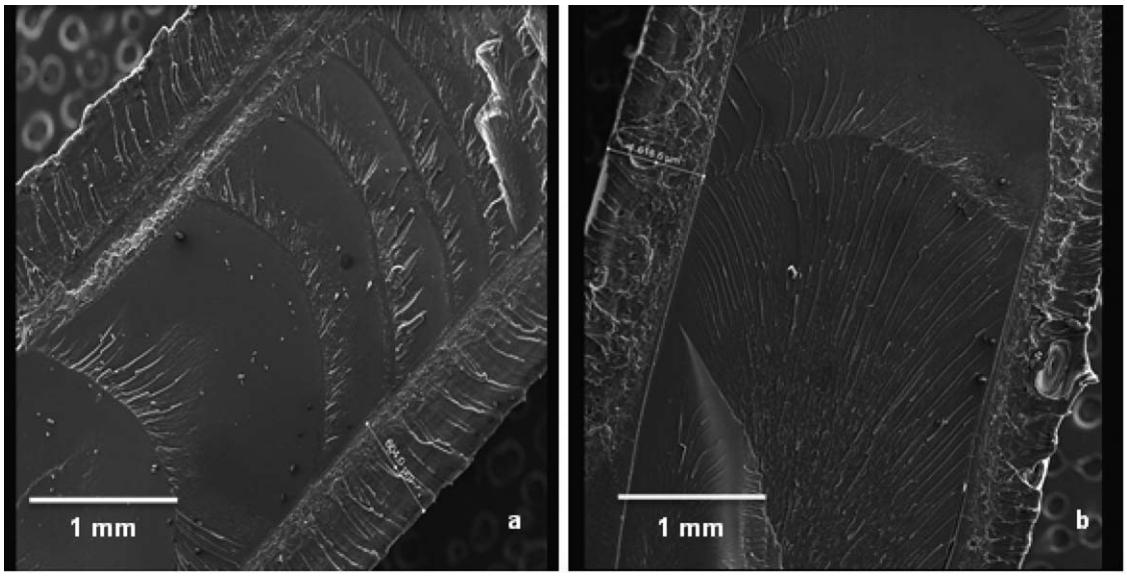


**Figure 4.** SEM images of notched impact samples at 80× magnification for: (a) 40/60% (PTT/PBT + PBS/PBAT) and (b) 60/40% (PTT/PBT + PBS/PBAT).

20% glass fiber as the core. Vangosa[14] similarly reported core temperature, and the interaction between core content and core injection rate as being statistically significant after a factorial analysis on co-injection processing parameters. Nagaoka et al.[11] varied injection speeds and determined that the significance of injection speed is dependent on the skin/core material combination, additionally, injection speed provided a much greater effect in sequential injection process over a single injection sandwich process (layered, mono-injection). This is likely because of the switch over period that occurs during sequential sandwich molding.[11]

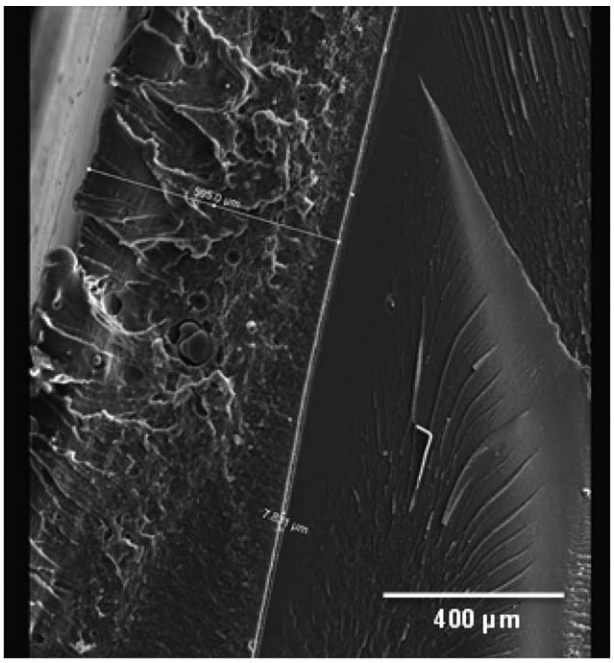


**Figure 5.** SEM image of notched impact sample at 200× magnification for 60/40% (PTT/PBT + PBS/PBAT).

### Notched Izod Impact

Impact strengths of the factorial DOE trials are displayed in Figure 2 along with the single injected PTT/PBT. It should be noted that the single injection of PBS/PBAT did not break under ASTM standards of any hammer size. The co-injected impact strengths which range from 450 to 95 J/m are considerably higher than the single injection of PTT/PBT with a max value of 25 J/m. The increased impact strength as a result of PBS/PBAT encapsulation has been previously reported by Zhang et al.[33] Impact strengths are compared to the average outer wall thickness of the impact sample, as to determine whether the large increases in notched impact strengths are because of skin/core adhesion, or simple a thicker core. If a thicker skin envelops the impact sample, upon notching the core will not be exposed to the hammer. In Figure 2 it can be seen that trial 2 produced the highest impact strength of the DOE experiments. Upon closer analysis of this result it is obvious that standard deviation has a large magnitude. This is a good indication that the skin thickness at the notch was close to the thickness of the notch, thus some samples would have had a notch with no core exposed causing the impact strength to increase dramatically as crack propagation initializing in the core and spreading to the skin would be minimized. Notched testing was also done on the samples formed from an injection ratio of 40 vol % skin and 60 vol % core, producing samples with lower skin/core ratios (Higher core content). The final results are displayed in Figure 3, and indicate that samples with lower skin content will display smaller impact values. To better understand if there was a trend between the skin thickness on the notched side and the impact strength a Pearson correlation analysis was done. When considering the correlation between the factorial impact strengths and the skin thickness there was a poor correlation

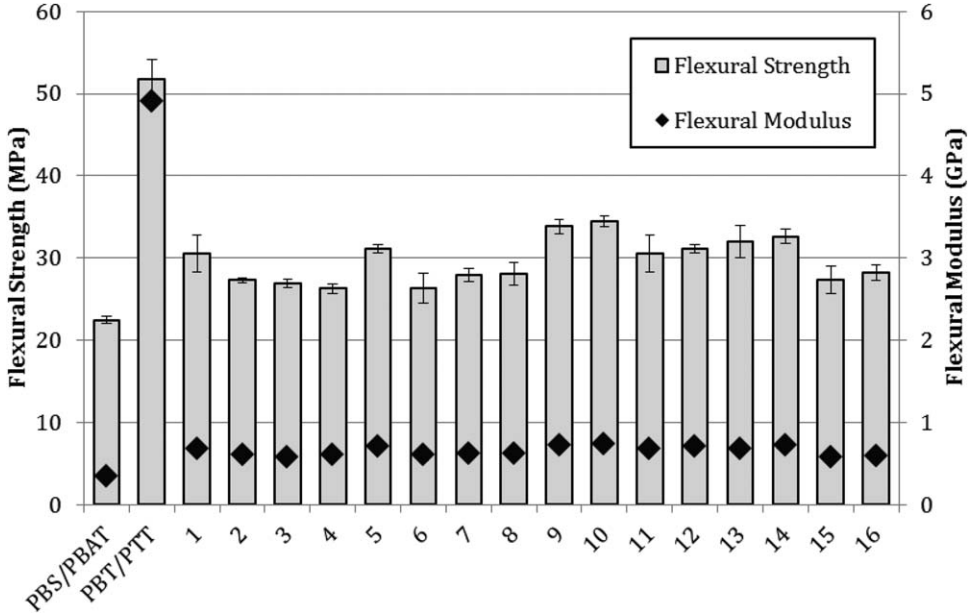


**Figure 6.** Flexural results of single injected PBS/PBAT, PTT/PBT, and co-injected factorial DOE trials of PTT/PBT (40 vol %) with PBS/PBAT (60 vol %). Refer to Table II for processing parameters of trials 1–16.

with a Pearson correlation of 0.110 and a *P*-Value = 0.685. When the results of the 60/40 trials impact strengths where added into the data set the correlation improved. Pearson correlation was 0.500 with a *P*-Value = 0.025, indicating that skin thickness has a positive correlation towards the co-injected impact strength and can be highly controlled by the skin/core ratios. The SEM images of both skin/core ratios are shown in Figure 4(a,b). In these images both brittle and ductile failure can be seen. Brittle failure is seen propagating from the impact point and through the sample specimen. Crack propagation becomes noticeably less advanced as it slows down while traveling through the core material. The ductile PBS/PBAT blend can be seen to undergo load transfer from the interface with the PTT/PBT core, more interestingly the direction of crack propagation for the ductile skin is perpendicular to the interface between the skin and core material. Looking at higher magnifications of the interfacial region PBS/PBAT shows the smaller rounded dislocations typical of ductile failure, before giving way to extended deformation as the crack propagates from the interface to the outer surface of the skin. Likewise from Figure 5 large dislocations running along the length of the skin/core interface are evident, before reconnecting further away from the initial impact point. The smoother fractioned surface of the PBS/PBAT near the impact point suggests a greater amount of energy was transferred from the core to the skin resulting in a more brittle like fracture for the skin. This higher energy transfer would have helped to contribute to the interfacial delamination.

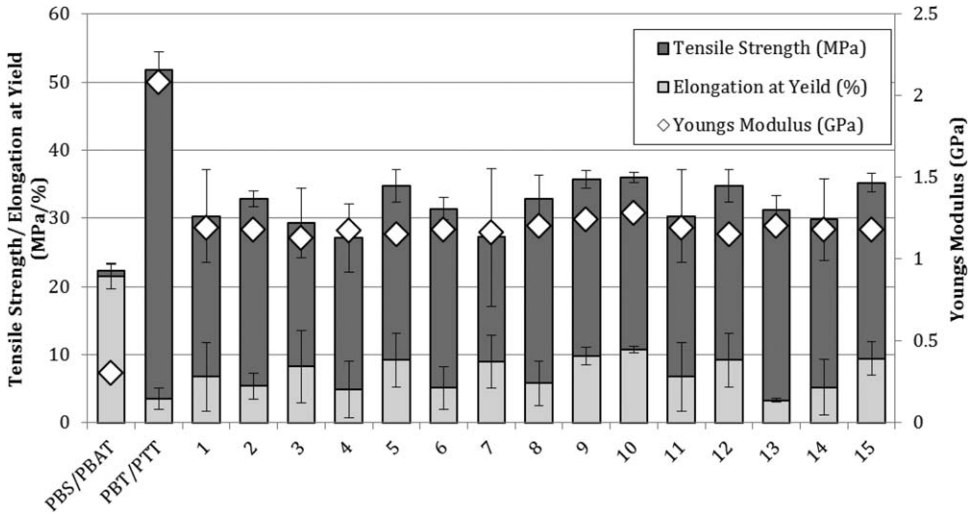


**Figure 7.** Tensile results of single injection of PBS/PBAT, PTT/PBT, and co-injected factorial DOE trials of PTT/PBT (40 vol %) with PBS/PBAT (60 vol %). See Table II for 1–16.

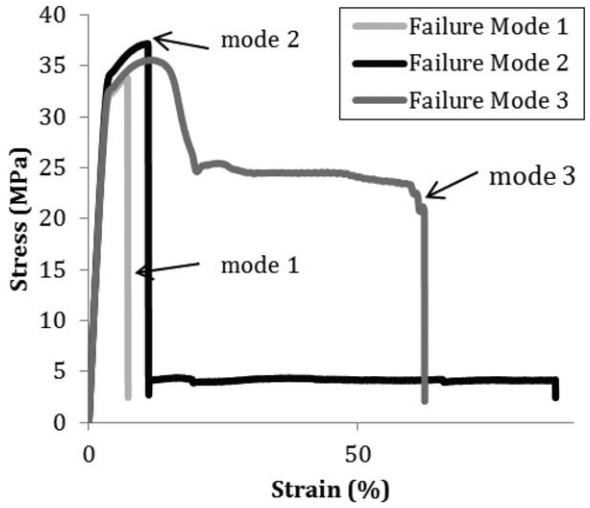


**Figure 8.** Three prominent modes of failure seen during tensile testing of co-injected factorial DOE trials. Failure mode 1 indicates lack of proper adhesion between PTT/PBT (70/30 wt %) and PBS/PBAT (60/40%). Failure mode 2 indicates better adhesion between PTT/PBT and PBS/. Failure mode 3 indicates the highest level of adhesion. Core polymer PTT/PBT undergoes full plastic deformation before extensive necking.

### Un-Notched Impact

By notching the impact samples a large defect is incurred along the continuity of the skin material. This in turn does not allow for a full understanding of the impact strength of the two dissimilar materials. To better understand the effect of co-injecting, un-notched impact samples are tested. For this test the impact processing method involving 60 vol % PTT/PBT (70/30 wt %) with 40 vol % PBS/PBAT (60/40 wt %) are used in an effort to test the thinnest possible skin layer. The samples failed to break under a 30 ft-lb hammer compared to pure PTT/PBT which shattered into many pieces under the 30 ft-lb hammer. From this data it can easily be said that the co-injection of PTT/PBT with PBS/PBAT helps offset the brittle nature of the PTT/PBT core.

### Flexural Results

Flexural strength and modulus are presented in Figure 6. Minimal variation in flexural results was recorded. Variation between trials was minimal with trial 10 at the highest 34.2 MPa and trial 4 at the lowest 26.2 MPa. The flexural modulus of the PBS/PBAT blend increased by 122% with the addition of PTT/PBT core. A 66% increase in flexural modulus with the addition of a high modulus core material has been previously reported with poly propylene as the skin and PP + 40% short glass fiber as the core,[21] 33% increase with PA 6 as the skin and PBT as the core.[8]

### Tensile Results

Tensile strength, modulus, and % of elongation at yield of the single injected PTT/PBT and the trials of the DOE are presented in Figure 7. Tensile strengths contained the same level of variation seen in flexural strength. Similarly to flexural strength, trial 10 had the highest tensile strength at 35.7 MPa and trial 4 had the lowest at 27.0 MPa. Since tensile testing presents an axial load on the co-injected sample, Young's modulus is likely to be a closer average of the two separate components, as opposed to flexural modulus which has a stress gradient that increases as the material becomes further from the neutral axis. The most intriguing response was percent of elongation at yield which was subjected to significant variation within each separate trial. The variations are considered to be linked to interfacial adhesion of the co-injected samples.[9] During testing the tensile samples could be grouped into three different categories relating to their mode of failure.

Figure 8 displays the stress–strain curves of three most common modes of failure. Some trials of the DOE displayed all three failure types within five samples. Failure mode 1 is shown to break at the end of the linear elongation with a % of elongation at

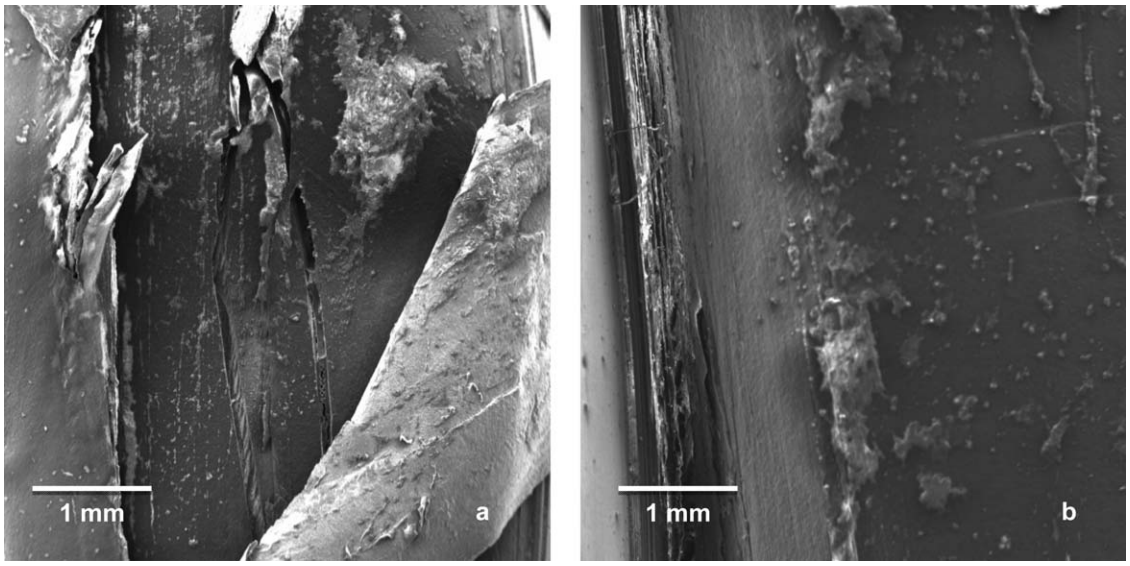


**Figure 9.** SEM images of surface of PTT/PBT core exposed by dissolving PBS/PBAT skin in chloroform. (a) Surface at 100× magnification. (b) At 100× magnification shows a large split on the left side running vertically.

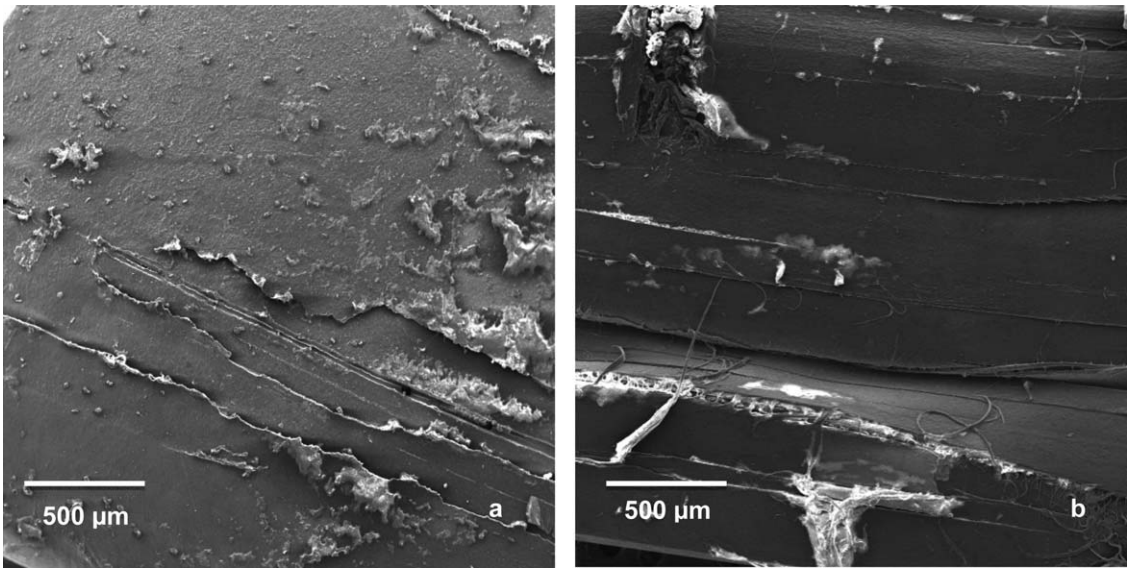


**Figure 10.** SEM images of co-injected PTT/PBT exposed by dissolving PBS/PBAT skin with chloroform after tensile testing. (a) Displays the surface of core PTT/PBT of a tensile sample after undergoing failure mode 1. (b) Displays the surface of core PTT/PBT of a tensile sample after undergoing failure mode 3.

yield < 3%. In this case the core material failed instantaneously with no necking visible. The skin material would often fully delaminate from the core and continue to be stretched. The second mode of failure contained the same linear elongation region but the core and skin maintained lamination before sudden core failure and delamination of the skin from the core. The % elongation at yield for this type of failure ranged from 3% to 8%. The last mode of failure had the highest % of elongation at yield with values greater than 8%. In this case the core and skin stayed laminated while the core underwent extensive necking before failing and becoming delaminated from the skin. No trend was seen in comparing tensile break modes to the processing parameters. It is thus proposed that the tensile failure mode must be an indication of randomly occurring mechanical interlocking between the polymer interfaces.

### SEM Images

To observe the potential mechanical interlocking between the skin and core blends SEM pictures were taken of the core PTT/PBT after PBS/PBAT had been dissolved off of co-injected tensile samples. Tensile samples taken from trial 10 which reported the greatest % elongation at yield with minimal standard deviation are used in the SEM images. Both Figure 9(a,b) display rough surface textures filled with voids and cracks. Figure 9(a) contains a large flap of the PTT/PBT material seen as the brighter band that covers the bottom right corner of the image. Figure 9(b) is another indication of extensive interlocking between the skin and core material. On the left side of Figure 9(b) image it is evident that there is a large separation within the core material. This split displays a high amount of texture, voids, and fibrillated polymer fibers suggesting that the skin and core had achieved mechanical intermeshing. Figure 10 displays the surface of the PTT/PBT core material from tensile tested materials. In Figure 10(a) the surface of a sample that underwent mode 1 failure is displayed. As expected the surface is relatively smooth with no indication of mechanical interlocking with PBS/PBAT. Figure 10(b) displays the surface of a sample that underwent mode 3 failure with extensive necking. In the wake of the dissolved skin a channel is visible on the surface of the skin, along with cracks and fibrous strands which suggest mechanical interlocking. While the processing parameter effects on the extent of skin/core interlocking are unknown it is considered that additional additives or fillers would regulate the mechanical interlocking and prove as useful modification in improving the % elongation at yield.

## CONCLUSIONS

This research investigated the feasibility and controllability of the co-injection a blend of PTT/PBT and PBS/PBAT in an effort to increase the scope of bio-polymer usage and add to the library of known compatible polymers for co-injection. The most promising effect was the increase in impact strength that was observed to increase with increasing skin (PBS/PBAT) thickness with values ranging from 56 to 450 J/m. Likewise samples with the thin skin profiles did not break in un-notched testing. Using a design of experiments for a factorial design allowed for a proper ANOVA analysis with interaction effects. The ANOVA results indicated that the interactions of melt(skin)*injection speed and melt(core)*injection pressure where prominent in most of the characteristic responses. This correlation indicates that a DOE is a good way to quickly map out the processing parameters effects on co-injection processability; however, it is largely dependent on mold shape. SEM images of notched Izod impact samples showed the brittle failure of PTT/PBT being hindered by the ductile failure of PBS/PBAT core, additionally the direction of failure in the skin layer was perpendicular to the impact head. Three different modes of failure during the tensile testing is a possible indication of mechanical interlocking which improves adhesion as seen in SEM images. In this case there is the potential for an additives or filler to be

used to increase the adhesion. This research indicates that the co-injection of PTT/PBT as a core material with PBS/PBAT as a skin material has a promising potential to be developed in to a final product with semi-biodegradable characteristics as well as contributing to a final material that improves upon the impact strength of pure PTT/PBT blends.

## ACKNOWLEDGMENTS

Authors are thankful to the financial supports from (1) highly qualified personnel (HQP) Scholarship from the Ontario Ministry of Agriculture, Food and Ministry of Rural Affairs (OMAF and MRA); Ontario, Canada; (2) OMAF/MRA – University of Guelph Bioeconomy industrial uses Research Program; (3) OMAF/MRA – New Directions Research Program; (4) the Ontario Ministry of Economic Development and Innovation (MEDI), Ontario Research Fund - Research Excellence Round 4 program; (5) Natural Sciences and Engineering Research Council (NSERC), Canada Discovery Grant individual (to Mohanty); and (6) NSERC NCE AUTO21, Canada.

## REFERENCES

1. Fischer, S.; Vlieger, J.; Kock, T.; Batenburg, L.; Fischer, H.MRS Proc 2000, KK2.2, 661.
2. Bhardwaj, R.; Mohanty, A. K.; Drzal, L. T.; Pourboghrat, F.; Misra, M. *Biomacromolecules* **2006**, *7*, 2044.
3. Siyamak, S.; Ibrahim, N. A.; Abdolmohammadi, S.; Yunus, A.; Wan, Md Z. B. W.; Rahman, M. Z. A.; *Molecules* **2012**, *17*, 1969.
4. Li, Y.; Shimizu, H. *Macromol. Biosci.* **2007**, *7*, 921.
5. Garner, P. J. Injection molding machines. U. S. patent 3 599 290 (**1971**).
6. Garner, P. J. Injection molding machines. U. S. patent 3690797 (**1972**).
7. Donovan, R. C.; Rabe, K. S.; Mammel, W. K.; Lord, H. A. *Polym. Eng. Sci.* **1975**, *15*, 774.
8. Selden, R. *Polym. Eng. Sci.* **2000**, *40*, 1165.
9. Gomes, M.; Martino, D.; Pontes, A. J.; Viana, J. C. *Polym. Eng. Sci.* **2011**, *51*, 2398.
10. Akay, G. *Polym. Comp.* **1983**, *4*, 256.
11. Nagaoka, T.; Ishiaku, U. S.; Tomari, T.; Hamada, H.; Takashima, S. *Polym. Test.* **2005**, *24*, 1062.
12. Vangosa, F. B. *Polym. Plast. Technol. Eng.* **2011**, *50*, 1314.
13. White, J L. *Polym. Eng. Sci.* **1975**, *15*, 481.
14. Young, S. S.; White, J. L.; Clark, E. S.; Oyanagi. Y. *Polym. Eng. Sci.* **1980**, *20*, 789.
15. Watanabe, D.; Ishiaku, U. S.; Nagaoka, T.; Tomari, K.; Hamada, H. *Inter. Polym. Process.* **2003**, *18*, 398.
16. Watanabe, D.; Ishiaku, U. S.; Nagaoka, T.; Tomari, K.; Hamada, H. *Inter. Polym. Process.* **2003**, *18*, 405.
17. Selden, R. *J. Injct. Mold. Technol.* **1997**, *1*, 189.
18. Zaverl, M. Seydibeyoğlu, O. Misra, M. Mohanty, A. *J. Appl. Polym. Sci.* **2012**, *125*, E324.
19. DuPont, [ONLINE] 2012 [ACCESSED] Nov 20, 2013. http://www.dupont.com/products-and-services/fabrics-fibers-nonwovens/fibers/articles/biobased-products.html.
20. Run, M.; Song, A.; Wang, Y.; Yao, C. *J. Appl. Polym. Sci.* **2007**, *104*, 3459.
21. Ahn, B.; Kim, S.; Yang, J. *J. Appl. Polym. Sci.* **2001**, *82*, 2808.
22. Yoo, S.; Im, S. S. *J. Polym. Sci. B Polym. Phys.* **1999**, *37*, 1357.
23. Huang, X.; Li, C.; Zheng, L.; Zhang, D.; Guan, G.; Xiao, Y. *Polym. Intern.* **2009**, *58*, 893.
24. Qiu, Z. B.; Ikehara, T.; Nishi, T. *Polymer* **2003**, *44*, 2503.
25. Qiu, Z. B.; Ikehara, T.; Nishi, T. *Polymer* **2003**, *44*, 3095.
26. Kim, Y. J.; Park, O. O. *J. Appl. Polym. Sci.* **1999**, *72*, 945–951.
27. Wu, C. S. *Carbon* **2009**, *47*, 3091 .
28. Ray, S.; Maiti, P.; Okamoto, M.; Yamada, K.; Ueda, K. *Macromolecules* **2002**, *35*, 3104.
29. Gua, S. Y.; Zhang, K.; Rena, J.; Zhan, H. *Carbohydr. Polym.* **2008**, *74*, 79.
30. Wenga, Y. X.; Jina, Y. J.; Menga, Q. Y.; Wanga, L.; Zhanga, M.; Wang, Y. Z. *Polym. Test.* **2013**, *32*, 918.
31. Coltelli, M. B.; Maggiore, I. D.; Bertoldo, M.; Signori, F.; Bronco, S.; Ciardelli, F. *J. Appl. Polym. Sci.* **2008**, *110*, 1250.
32. John, J.; Mani, R.; Bhattacharya, M. *J. Polym. Sci. A Polym. Chem.* **2002**, *40*, 2003.
33. Zhang, K.; Nagarajan, V.; Zarrinbakhsh, N.; Mohanty, A. K.; Misra, M.; *Macromol. Mater. Eng.* **2013**, *298*, 1.
34. Baltus, W.; Carrez, D.; Carus, M.; Kaeb, H.; Ravenstijn, J.; Zepnik, S. Market study on Bio-based Polymers in the WorldCapacities, Production and Applications: Status Quo and Trends towards 2020 Nova-Institute 2013.
35. Messaoud, D.; Sanchagrin, B.; Derdouri, A. *Polym. Comp.* **2005**, *26*, 265.
36. Kadota, M.; Cakmak, M.; Hamada, H. *Polymer* **1999**, *40*, 3119.